A Survey on MIMO/CF MIMO Algorithm Development

Joseph Kuo
jokuo@ucsd.edu

Andrew Liu
anl078@ucsd.edu

Stephen Wilcox
swilcox@ucsd.edu

I. Introduction and Motivation

The rapid evolution of wireless communication systems has placed increasing demands on the capacity, reliability, and efficiency of networks. Multiple Input Multiple Output (MIMO) architectures have emerged as one of the most trans-formative technologies in addressing these demands. By leveraging multiple antennas at the transmitter and receiver, MIMO systems exploit spatial diversity and multiplexing gains to significantly enhance data throughput, spectral efficiency, and link reliability. This project is motivated by the desire to push existing MIMO design to new limits [1]. By conducting a thorough survey of existing MIMO architectures, the project aims to identify key beneficial trends in certain designs and uncover potential areas for further improvement. This endeavor will not only advance the academic discourse but also contribute to practical advancements in the design and deployment of next-generation communication systems.

II. Comparison with Other Related Works

A. Background

Network planning for wireless networks is essential to provide a high data rate and capacity network [2]. The focus of the project will be based on the ideas covered by DenseQuer, a project that replaces a single high-power base-station with multiple smaller, low-power ones. These smaller base stations reduce the total power usage for wireless communication, which can scale tremendously over base station deployments over massive areas. However, DenseQuer is limited to the SISO system [3], so part of the project will be applying the design towards MIMO. It should be noted that in MIMO, a converse approach to DenseQuer exists in the form of massive MIMO by grouping large amounts of antennas at the transmitter and receiver, generally boasting good coverage and energy efficiency [4]. However, the deployment of these kinds of structures is very costly in terms of equipment and power upkeep; in addition, the transmitter has a demanding design for any application involving low-band, effectively limiting it to high frequency applications which suffer from issues with propagation distance and lack of line-of-sight. To address some of these difficulties, development in cell-free MIMO was explored, where the distribution of APs is spread throughout an area and with intentional overlap between cells, designed to cover the same area as a massive MIMO system while making the quality of the network coverage more uniform across the area. In this way, issues that result from operating on cell-edges or general LoS are reduced by dispersing the location of APs so that the user is mostly centralized in the cluster [5]. Improvements upon this concept have been made to make this coverage more dynamic; a proposal for user-centric CF-MIMO suggests how serving clusters can be dynamically created to ensure that connection quality stays consistent as a user moves through an area. It should be noted that the main difficulties of this approach lie mainly in how to best optimize the distribution and size of the network, as cell-free MIMO still deals with the same issues in terms of power-upkeep and maintenance as massive MIMO for its APs (compounded with increased intercellular interference as AP deployment increases); the population in the areas CF-MIMO must be optimized in is often much more varied than with traditional coverage map constructions, thus the process of selecting and configuring sites to best provide users with seamless connections is an ongoing issue [5]. Thus, our approach is to use Sionna [6] to optimize the placement of base stations for a CF-MIMO network in urban environments to better suit communication involving mobile/low power IOT devices. We will run simulations in NVIDIA Sionna to verify that our MIMO structure increases the power efficiency of the base stations.

III. Directly Related Works

Our approaches to certain design decisions can be observed in the following papers:

- "Densify and Conquer": A study performed using SISO comparing the carbon footprint of sparse high power base stations to low power densely dispersed transmitters over the same coverage area. The framework behind Tx positional placement was sourced from this paper.
- "User-centric cell-free massive MIMO": A survey of development and existing challenges in CF-massive MIMO; highlights the importance of developing user allocation algorithm to serving clusters to optimize Quality of Service (QoS). This paper established the focus of the project to be on achieving consistent channel quality (channel hardening and energy efficiency), as the parameters mentioned were outlined as imperative for the success of a CF MIMO system.
- "Analysis of the Impact of Antenna Arrangement on System Capacity of MU-MIMO": A paper that explores optimal antenna array design to best support terminal

mobility in MIMO (handover between networks/changing point of attachment). This paper informed the transmitter design of the planar arrays in the Sionna simulation

IV. Design

In our project, we aim to analyze how different transmitter and receiver configurations impact coverage across a given area. To achieve this, we will explore various base station configurations, simulating how signals propagate from the base stations to different locations on the map. In these simulations we will vary the location, antenna configurations, and transmitter heights. This approach allows us to assess coverage variations and gain insight on optimized deployment strategies.

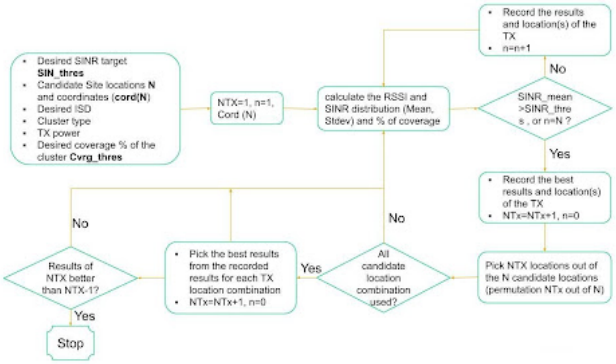

Fig. 1. Design Process

V. Implementation

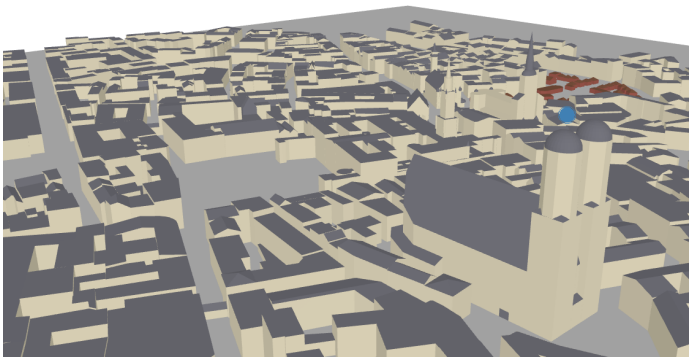

Fig. 2. The Munich scene from Sionna. The blue dot represents a transmitter placed onto the scene.

In our project we use a python library from NVIDIA called Sionna [6]. Sionna is an open-source library made for link-level simulations that allows developers to rapidly prototype complex communication systems. Sionna features realistic ray tracing and propagation algorithms that can be used to simulate signal propagation from a transmitter(TX) to a receiver(RX). This is implemented in their coverage_map function, which uses a scene which is a 3D map with one or many transmitters placed onto the it and it computes the estimated received signal strength (RSS) from the various transmitters for every position in the map. When computing the RSS, the simulation models signal propagation from transmitters to various locations, accounting for reflections off the map geometry up to the max_depth limit. The result is a coverage_map, which has metrics like path gain, SINR, and RSS for the the entire map.

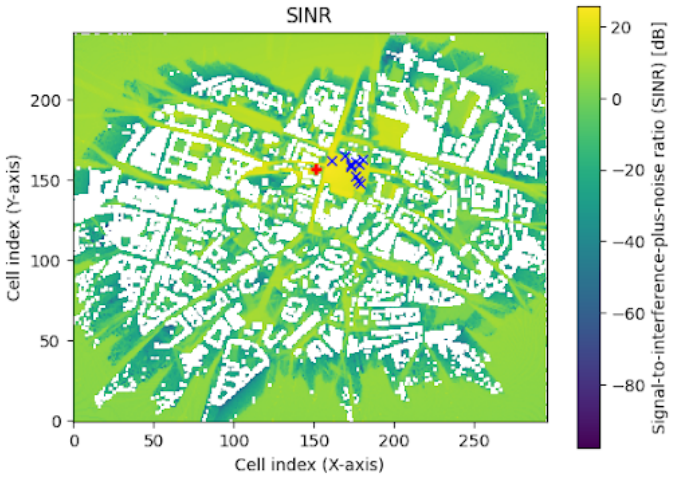

Fig. 3. A Sionna coverage map. The red cross represents the transmitter location and the blue X's show the points that were sampled.

Before starting any MIMO simulation, we must first verify that the SINR of the received signal increases proportionally to the number of antennas, approximately by a factor of N as the number of antennas increases by N times. To validate this, we set up a single transmitter at a fixed location with a varying number of antennas. We configured a planar antenna array, adjusting the number of rows and columns to control the total number of antennas. We then used the built-in coverage map function in Sionna to analyze SINR distribution across the area.

Points	1	2	3	4	5	6	7	8	9	10
iso_64	11.37	32.05	38.44	-20.51	9.43	0.11	-14.48	31.01	36.38	28.39
iso_16	28.11	31.60	33.24	-6.77	27.96	26.43	2.09	32.05	33.37	30.46
iso_1	23.44	21.17	21.49	-17.68	20.63	20.10	-6.12	21.92	22.36	20.71
tr_64	18.16	39.78	46.40	-13.31	16.56	7.22	-9.47	38.69	44.56	36.02
tr_16	34.91	39.33	41.20	1.06	35.19	33.50	5.06	39.72	41.20	38.07
tr_1	30.23	28.90	29.41	-8.39	27.80	27.14	3.68	29.59	30.13	28.31
dipole_64	12.75	33.74	40.19	-19.85	10.97	1.74	-12.52	32.68	38.42	30.09
dipole_16	29.50	33.30	34.99	-5.58	29.62	28.05	1.00	33.70	35.12	32.15
dipole_1	24.83	22.87	23.21	-14.46	22.29	21.71	-5.80	23.57	24.14	22.40

Fig. 4. Table showing the SINR values of the points from Fig. 3

Since many locations on the map are obstructed by buildings and receive no signal, we could not randomly select test points from the entire area. Instead, we restricted our selection to locations near the transmitter to ensure valid SINR measurements. As shown in Fig. 3, the red "+" masks the transmitter location, while the blue "x" marks the randomly selected point on the coverage map. To further analyze SINR variations, we experimented with different antenna types. including isotropic, dipole, and tr38901.

In Sionna, the entire coverage map is divided into multiple rectangular cells, with each cell's size controlled by the "cell_size" parameter. Each cell is indexed by its (i, j) coordinates, allowing us to extract SINR values at specific locations. For example, the point (158, 173) refers to a particular cell on this grid where we analyze SINR variations.

In Fig. 4, the labels indicate different configurations:

- **iso** is for isotropic antennas
- **tr** is for tr38901 antennas
- **dipole** is for dipole antennas

The suffix indicates the number of antennas used on the transmitter.

In Sionna, SINR is computed using the received signal strength (RSS) and the interference-plus-noise power. The received signal strength at a given cell (i,j) is given by: $RSS_{i,j} = P_{tx} \cdot g_{i,j}$ where P_{tx} is the transmitted power in Watts and $g_{i,j}$ represents the path gain, which accounts for the factors such as signal attenuation, reflections, and diffraction. For a scene with multiple antennas, the SINR of the transmitter k at a given cell is computed as

$$\text{SINR}_{i,j}^{k} = \frac{\text{RSS}_{i,j}^{k}}{N_0 + \sum_{k' \neq k} \text{RSS}_{i,j}^{k'}}$$

N_0 is the thermal noise power in Watts and it is calculated as $N_0 = B \cdot T \cdot k$ where B being the transmission bandwidth, T the temperature, and k is Boltzmann's constant.

Apart from the number of antennas, SINR is influenced by multiple factors, including:

- **Signal reflections and diffraction** due to environmental obstructions,
- **Interference** from other transmitters in multi-transmitter scenarios,
- **Thermal noise power**, which depends on system temperature and bandwidth.

By analyzing the extracted SINR values, we observe a clear trend of increasing SINR as the number of antennas at the transmitter increases. Specifically, at multiple selected locations, the SINR follows this pattern. For instance, at one measurement point (158, 173) using an isotropic antenna:

- With 1 antenna (iso_1), the SINR is 21.49 dB.
- With 16 antennas (iso_16), the SINR increases to 32.24 dB.
- With 64 antennas (iso_64), the SINR further increases to 38.44 dB.

Since SINR in decibels follows the relationship SINRdB = 10*log10(SINR), an increase of approximately 10 dB corresponds to a 10 times increase in the linear SINR values.

From observing the SINR increments we can see: Increasing from 1 to 16 antenna results in an SINR increase of (33.24-21.49) = 11.75 dB, which closely aligns with the theoretical prediction of 10*log10(16) = 12 dB. Increasing from the 16 to 64 antenna results in an SINR increase of (38.44 - 33.24) = 5.2 dB, which is close to 10*log10(4) = 6 dB. A similar trend is observed at other measurement points across different antenna types, as shown in the extracted data. For example, at another point (160, 173), the SINR values for iso_1, iso_16, and iso_64 are 22.36 dB, 33.37 dB, and 36.68 dB, respectively. This pattern holds across different antenna configurations, including dipole and tr38901 antennas.

However, due to real-world effects such as signal reflections, obstructions, interference, and multipath fading, not all points on the map experience an SINR improvement exactly by a factor of N. While the overall trend supports the theoretical expectations, some locations may have deviations due to complex propagation conditions. These variations are especially noticeable in dense urban environments where buildings and other obstacles impact signal strength and interference patterns. These results confirm the expected MIMO gain, demonstrating that across multiple measurement points, SINR improves approximately by a factor of N (in linear scale) as the number of antennas increases by N times, though real-world imperfections may cause deviations.

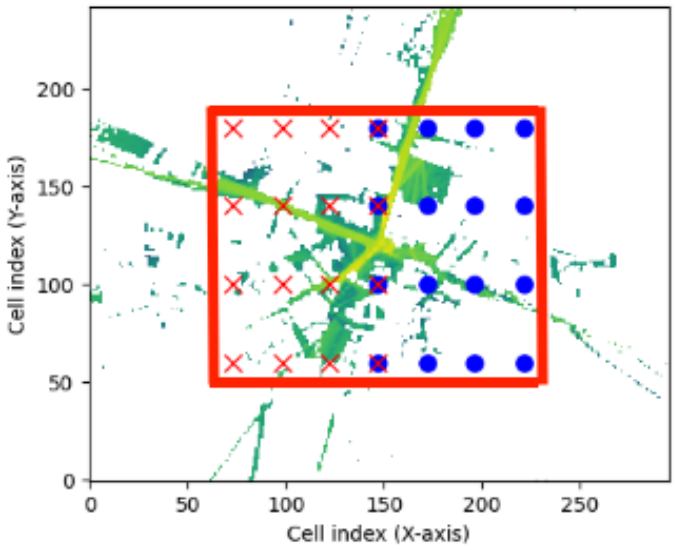

Fig. 5. Configurations of the transmitter positions in the Dynamic Uniform Distributed TX scenarios.

In our MISO simulations, we are interested in exploring the impact of network densification and to do this we explore various configurations:

- **Centralized TX**: The transmitters are placed near the center (Fig. 7) and the look_at is varied as shown in Fig. 6.
- **Static Uniform Distributed TX**: The map is split in into blocks and a transmitter is placed in the center of each block (Fig. 7). The look_at is varied as shown in Fig. 6.
- **Dynamic Uniform Distributed TX**: (Uniform Densification) The center of the map is divided into 2 sections, each containing 16 locations that a transmitter can be at as shown in Fig. 5. For each transmitter, each location is tested with an isotropic signal and default orientation(i.e. [0,0,0]), and out of these locations, the ones with the best coverage are chosen. The transmitters then loop through the look_at grid shown in Fig. 6.

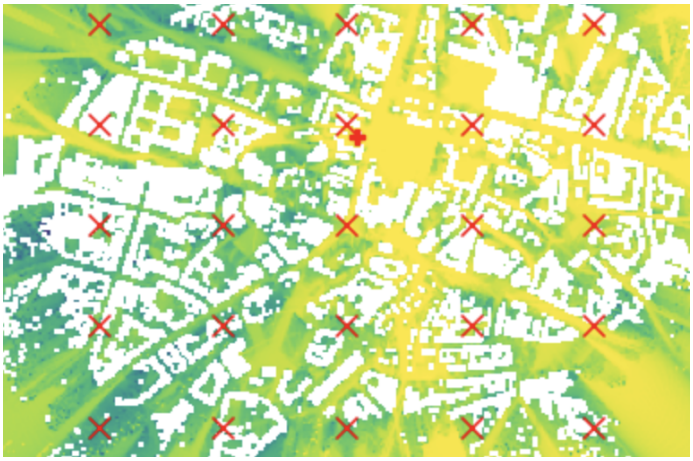

Fig. 6. The X's show the various look_at positions used in the centralized and evenly distributed TX simulations.

A key metric used to evaluate the performance of each network densification is coverage. Coverage is determined by counting the total number of cells in the coverage map that exceed a certain threshold. We use the SINR values extracted from the coverage map and set a 5 dB SINR threshold to assess coverage. Cells with SINR above 5 dB are of particular interest, as they indicate a good, more reliable signal that is suitable for stable communication.

To determine the coverage for multiple transmitters, we first process the SINR data for each individual antenna. We convert all blocks or elements in the coverage map into a binary matrix, where "true" values indicate that the corresponding blocks have an SINR value that is above 5 dB. Note that the SINR values extracted from the coverage map function are stored as a 3D dataset, with the following dimensions:

- The first dimension represents the **number of transmitters**.
- The second dimension corresponds to the **cell index along the y-axis** of the coverage map.
- The third dimension corresponds to the **cell index along the x-axis** of the coverage map.

To analyze the SINR for individual transmitters, we extract data from the first dimension, converting it into a 2D matrix for each transmitter. After extracting the relevant data, we perform a logical OR operation across multiple SINR matrices from different transmitters to compute the overall coverage for multiple transmitters. Using an OR operation allows us to capture the union of all coverage areas, ensuring that we account for all locations served by at least one transmitter.

However, this method represents a theoretical calculation that does not account for interference between transmitters. We assume that the precoding vectors and combining vectors for each transmitter are optimized correctly, ensuring no interference between them.

Another important parameter in our design is the "look_at" position of the transmitters, which determines the direction of the transmitted signal. By adjusting the "look_at" position, we can further enhance the coverage of the transmitters and improve overall network performance. As mentioned earlier, total coverage is calculated using a logical OR operation across individual transmitter coverage areas. To maximize coverage, we need to steer each transmitter in different directions to minimize overlap and ensure that their coverage areas complement rather than interfere with each other. To search for the optimal "look_at" positions. We first calculate the individual coverage for each look_at positions (in Fig 5.) for all transmitters . Then, we find the best combination of "look_at" positions for all transmitters that maximizes total coverage by evaluating all possible permutations of the look_at positions across all transmitters.

In uniform densification, we observed that as the transmitter height decreases, its placement becomes increasingly important. A lower transmitter height increases the likelihood of it being surrounded by buildings, which can significantly reduce its coverage. To address this issue, we introduced a strategic approach to optimize transmitter placement while reducing the transmitter height to 17 meters.

The primary objective of this approach is to identify optimal locations for multiple transmitters in a dense urban environment with numerous buildings. From the results of centralized and distributed densification, we found that uniform densification achieves better coverage performance.

Additionally, as observed in Fig. 3, the four corners of the coverage map lack buildings. To enhance transmitter placement efficiency, we exclude these regions by defining a boundary box, restricting where transmitters can be placed. Within this boundary, the coverage area is uniformly divided into N smaller rectangular blocks, where N is determined by the number of transmitters.

Within each block, designate 16 potential transmitter locations for the transmitter associated with the given block. For example, in the case of two transmitters, the possible locations for Transmitter 1 are marked as red "x", while the possible locations for Transmitter 2 are marked as blue "o", as shown in Fig. 36. Note that due to our limited computational power we limited the number of positions for the transmitters and we also limited the testing to only isotropic antennas. As a result, we were able to break down the optimization into a two-step process, rather than treating it as a joint optimization problem with two control variables (transmitter location and "look_at" direction). This simplification significantly reduces the complexity of the optimization while still allowing us to explore a meaningful subset of the design space.

With this setup, we can now search for the optimal transmitter locations. We first calculate the individual coverage for each potential transmitter location. Then, to find the best combination of transmitter placements that maximizes total coverage, we evaluate all possible permutations of candidate locations across transmitters.

For example, if each of the N transmitters has 16 possible locations, the total number of combinations to evaluate is 16^N. This combinatorial search ensures that we consider all possible placement configurations to find the one that yields the highest

overall coverage. However, due to computational constraints, we limit the number of candidate locations and apply efficient evaluation strategies to make the optimization tractable.

Once the transmitter locations are optimized, we proceed to optimize the look-at position for each transmitter to further enhance signal directionality and overall performance.

For our MIMO simulations, we build upon the MISO simulations by adjusting the number of receiver antennas. This is possible because Sionna's simulation framework allows flexible configuration of antenna arrays without requiring fundamental changes to the propagation modeling. Since we are investigating Cell-Free MIMO, we chose to design the receiver with 4 antennas, considering that most modern mobile devices are equipped with multiple antennas for enhanced signal reception.

VI. Evaluation

The analysis focuses on two key metrics: (1) the maximum overlap of coverage blocks, which indicates the optimal spatial alignment of transmitters for maximum coverage, and (2) the maximum Signal-to-Noise Ratio (SINR) achieved in the map, which reflects the quality of the communication link. Additionally, the number of blocks above a predefined SINR threshold is reported, providing insight into the system's reliability and coverage efficiency. Note that "Dynamic" distributions refers specifically to transmitter positions tested in the Dynamic Uniform Distributed transmitter scenarios (see Fig. 7).

Config.	Num. Tx	Dist.	Height(m)	Area	Max. SINR(dBm)
MISO	2 Tx	Centr.	50	9448	31.43
MISO	2 Tx	Centr.	20	1043	36.67
MISO	2 Tx	Distr.	50	11173	30.40
MISO	2 Tx	Distr.	20	2309	37.10
MISO	4 Tx	Centr.	50	13993	29.71
MIMO	4 Tx	Centr.	20	7208	37.76
MISO	4 Tx	Distr.	50	25795	28.86
MISO	4 Tx	Distr.	20	2763	35.34
MISO	2 Tx	Dyna.	20	6414	37.66
MISO	4 Tx	Dyna.	20	10160	34.22
MIMO	2 Tx	Centr.	50	9464	31.43
MIMO	2 Tx	Centr.	20	1043	36.67
MIMO	2 Tx	Distr.	50	11115	30.39
MIMO	2 Tx	Distr.	20	2299	38.84
MIMO	4 Tx	Centr.	50	19331	35.37
MIMO	4 Tx	Distr.	50	32373	34.26

TABLE I
Results

From the results outlined in Table 1 and the coverage maps we obtained (refer to the "Extra Figures" section for relevant coverage maps) we see that changes in each parameter produce results that we would roughly anticipate observing with transmitters in reality.

As expected, the distributed transmitters were able to cover a larger area than the centralized transmitters during the simulations in both MISO and MIMO cases. The ratios between total coverage began to show an increased disparity as more transmitters were added and the height of transmitters was modified. For example, the two-transmitter coverage ratio between the two deployment schemes at a transmitter height of 50 m was 117.4%; this ratio increased to 220% when both heights were decreased to 20 m. indicating that distributed placement had much better scalability than centralized placement when deploying transmitters with line-of-sight restrictions. We observe a similar pattern occur when keeping the transmitter height static but increasing the number of transmitters deployed for each distribution. This served as a reaffirmation of results found in the prior CF survey papers we read, as well as highlighting transmitter height as important metric that an algorithm using this framework should account for. However, it should be noted that the maximum SINR recorded by simulation was slightly higher for centralized schemes compared to distributed schemes when the height remained at 50 m, indicating that average performance across the coverage area for centralized schemes was slightly higher. As such, it is important for an algorithm to be able to operate based off a predetermined consideration of how transmitter deployment might be constrained and what the intended area of coverage might be.

Our rudimentary design of a dynamic distribution algorithm for coverage was successful as well, as we were able to produce maximum SINR measurements and total coverage area that exceeded the measurements we had for the static central and distributed transmitter positions we had. This is only directly observable for the cases where transmitter height was 20 m, though we feel that this demonstration is sufficient enough to justify the design of a more greedy algorithm that can iterate over an increased location pool to determine optimal transmitter placements.

An interesting pattern we observed was that the coverage between MISO and MIMO was roughly equivalent at lower transmitter heights for the same deployment schemes. This is more of an arbitrary detail as the focus of the project was designed for creating a simulation framework for MIMO specifically, though it does inform us how this algorithm might lend itself to the design of scalable MISO IoT network applications, where we can expect limitations in the design of the user devices as well as the network itself. For replication purposes, it should also be stressed that these results were obtained using transmitter deployments that had pre-defined optimal positions as well as pre-set heights due to limitations on our computational power; the main purpose of this framework is a proof of concept for future design. A true, greedier iterative algorithm might identify alternate positions based on distance thresholds to differentiate between the distribution schemes (ex: transmitter must be at least x distance apart to be considered distributed) or other constraints that may be defined. The number of transmitters for each case was also defined primarily to demonstrate the ability of the algorithm to assess scalability, as the actual number of optimal transmitters determined by a more robust simulation model will differ between environments.

VII. Conclusion/Future Work

From our results, we can conclude that the design of a computational algorithm for optimizing a CF-MIMO network is very possible, if not feasible, with the metrics we identified in our simulations. The framework for optimizing a low-power widely distributed network was demonstrated by our work, though we feel that the constraints we had with our simulations limited our capacity for implementing potential designs around this framework. To be precise, our limited computational power which prevented us from running comprehensive simulations, so future work would involve securing access to a computer with multiple GPU's to allow accelerated ray-tracing. With the increased computing power, we would improve our results by increase the size of the potential transmitter position grid to be similar to the number of cells in the map so every position can be tested along with increasing the size of the look-at grid and looping through it for each transmitter. By doing this we can simulate each transmitter to cover as much area as possible with as little interference to other transmitters, and run more robust iterative processes to optimize network performance.

VIII. Individual Contribution

Joseph:

Joseph wrote most of the code for the generating and comparing the different base station configurations. He also helped with analyzing the results, maintained consistent communications with the team and contributed to the proposal, reports, and presentation.

Andrew:

Andrew did most of the research and a lot of the writing for the proposal, reports, and presentation. He also helped with analyzing our results and maintained consistent communication with the team.

Stephen:

Stephen helped with writing and simulating the code, and with analyzing the results. He also maintained consistent communication with the team and contributed to the proposal, reports, and presentation.

References

[1] K. N. R. S. V. Prasad, E. Hossain, and V. K. Bhargava, "Energy efficiency in massive mimo-based 5g networks: Opportunities and challenges," *IEEE Wireless Communications*, vol. 24, no. 3, pp. 86–94, 2017.

[2] R. Q. Shaddad, F. S. Al-Kmali, M. A. Noman, N. K. Ahmed, E. M. Marish, A. M. Al-Duais, A. Ali Al-Yafrsi, and F. A. Al-Sabri, "Planning of 5g millimeterwave wireless access network for dense urban area," in *2019 First International Conference of Intelligent Computing and Engineering (ICOICE)*, pp. 1–4, 2019.

[3] A. Gupta, A. Heidari, J. Jin, and D. Bharadia, "Densify conquer: Densified, smaller base-stations can conquer the increasing carbon footprint problem in nextg wireless," 2024.

[4] L. Lu, G. Y. Li, A. L. Swindlehurst, A. Ashikhmin, and R. Zhang, "An overview of massive mimo: Benefits and challenges," *IEEE Journal of Selected Topics in Signal Processing*, vol. 8, no. 5, pp. 742–758, 2014.

[5] M. Hoffmann and P. Kryszkiewicz, "Evaluation of user-centric cell-free massive multiple-input multiple-output networks considering realistic channels and frontend nonlinear distortion," *Applied Sciences*, vol. 14, p. 1684, 02 2024.

[6] J. Hoydis, S. Cammerer, F. Ait Aoudia, M. Nimier-David, L. Maggi, G. Marcus, A. Vem, and A. Keller, "Sionna," 2022. https://nvlabs.github.io/sionna/.

IX. Extra figures

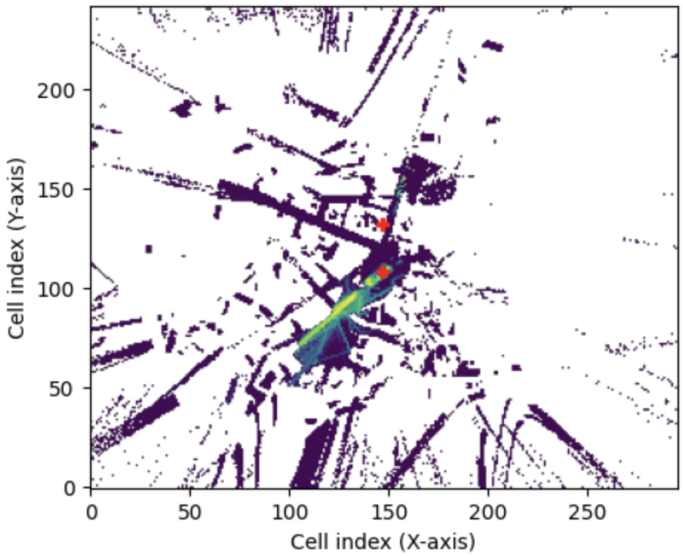

Fig. 7. Configurations of the transmitter positions in the Centralized TX scenarios.

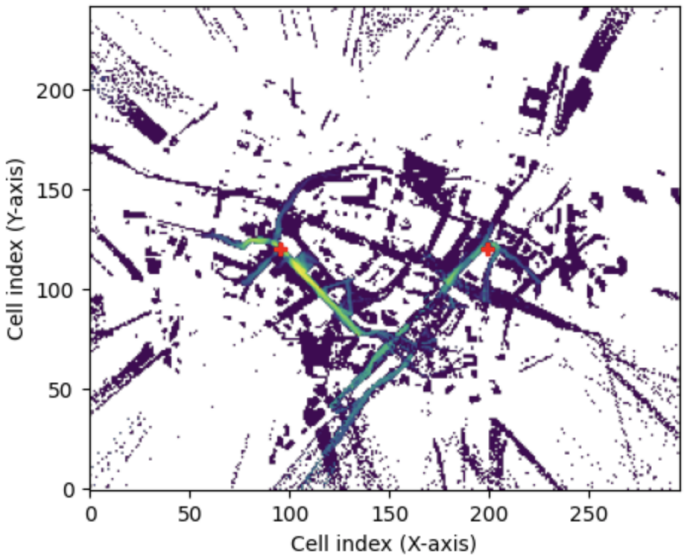

Fig. 8. Configurations of the transmitter positions in the Static Uniform Distributed TX scenarios.

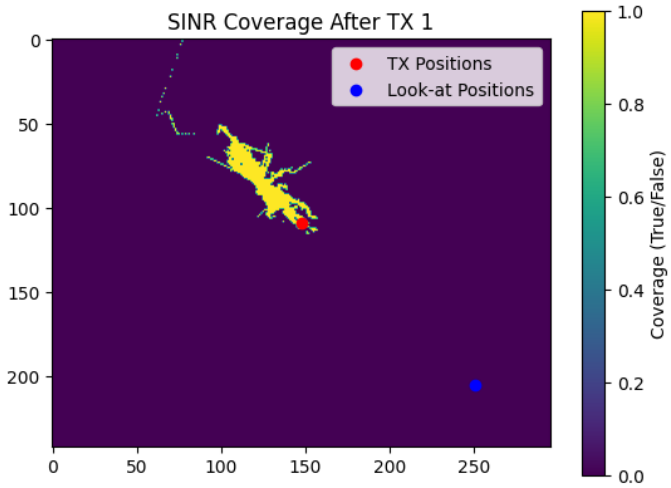

Fig. 10. Theoretical SINR coverage of MISO Centralized 2TX at first iteration, TX Height = 20m

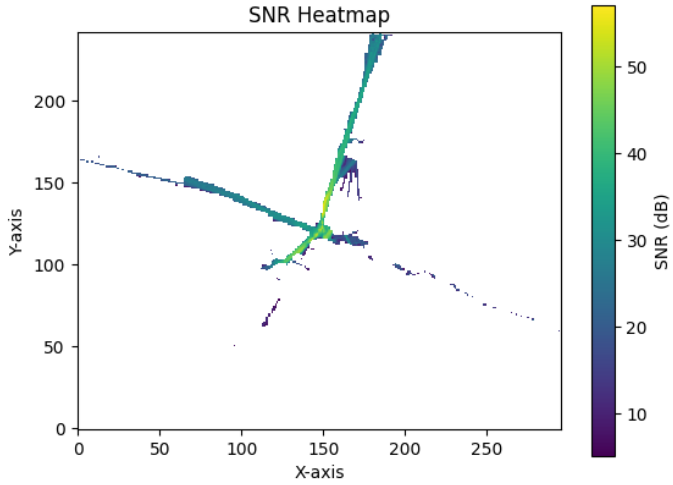

Fig. 9. FINAL SINR coverage of SISO 1TX from Sionna, TX Height = 20m

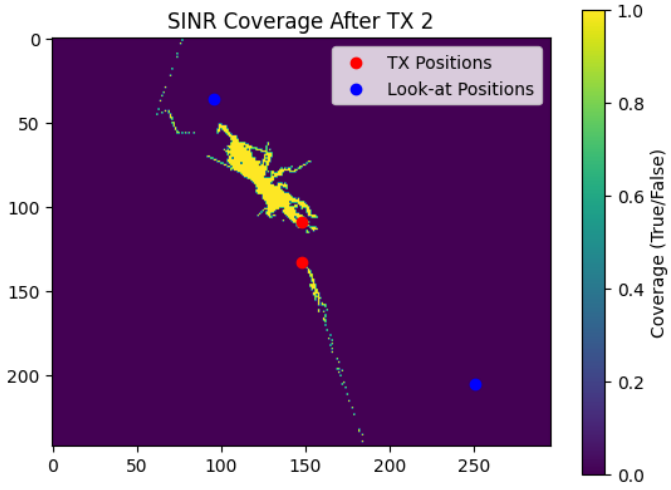

Fig. 11. Theoretical SINR coverage of MISO Centralized 2TX at second iteration, TX Height = 20m

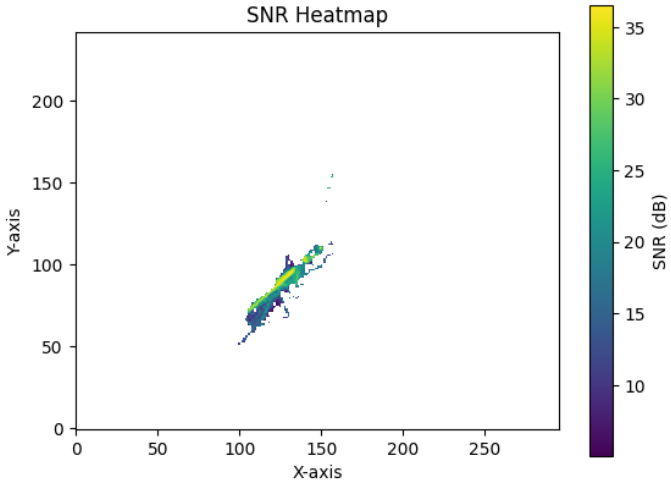

Fig. 12. FINAL SINR coverage of MISO Centralized 2TX from Sionna, TX Height = 20m

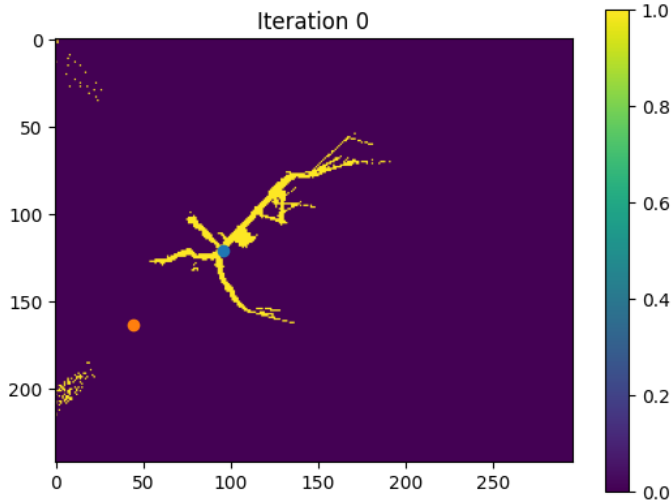

Fig. 13. Theoretical SINR coverage of MISO Uniform Distributed 2TX at first iteration, TX Height = 20m

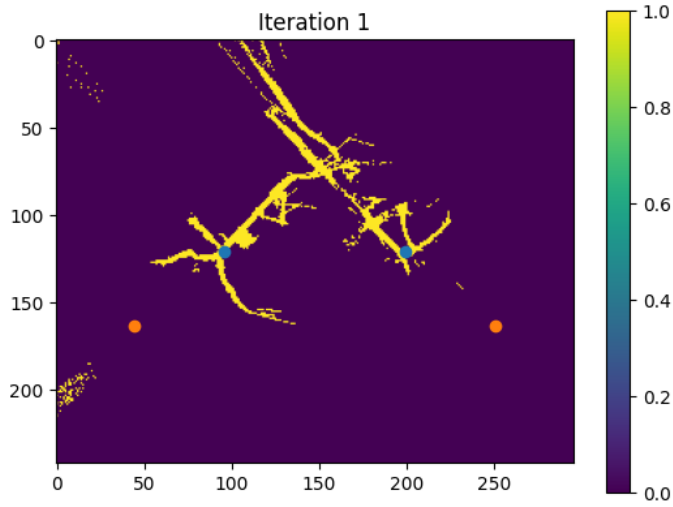

Fig. 14. Theoretical SINR coverage of MISO Uniform Distributed 2TX at second iteration, TX Height = 20m

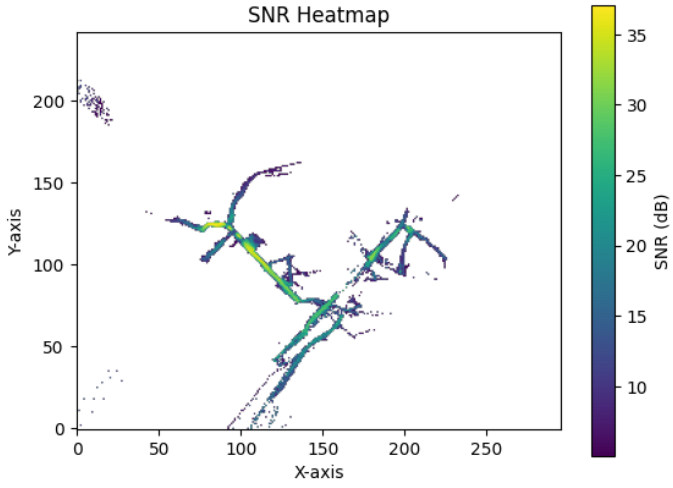

Fig. 15. FINAL SINR coverage of MISO Uniform Distributed 2TX from Sionna, TX Height = 20m

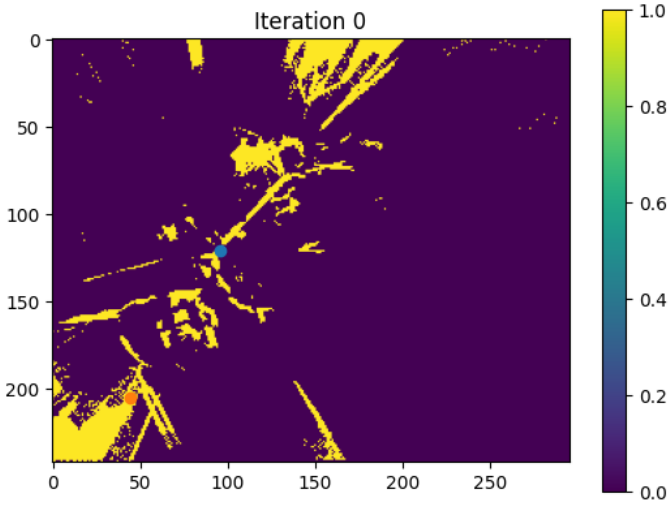

Fig. 16. Theoretical SINR coverage of MISO Uniform Distributed 2TX at first iteration, TX Height = 50m

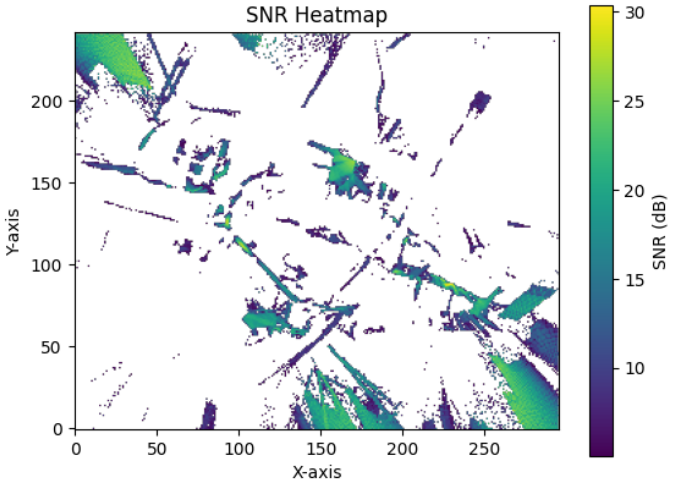

Fig. 18. FINAL SINR coverage of MISO Uniform Distributed 2TX from Sionna, TX Height = 50m

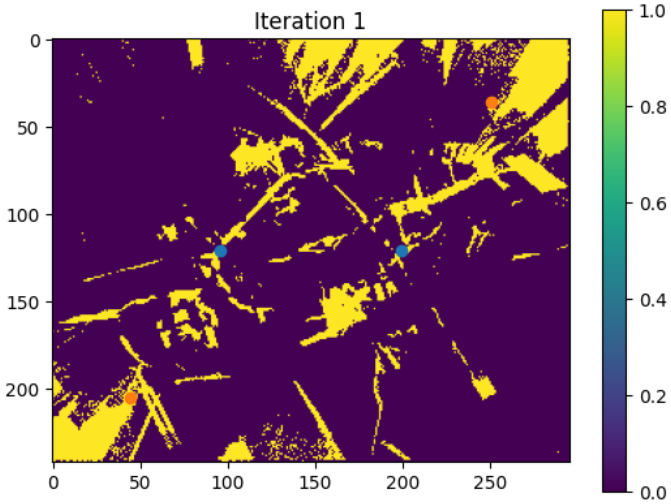

Fig. 17. Theoretical SINR coverage of MISO Uniform Distributed 2TX at second iteration, TX Height = 50m

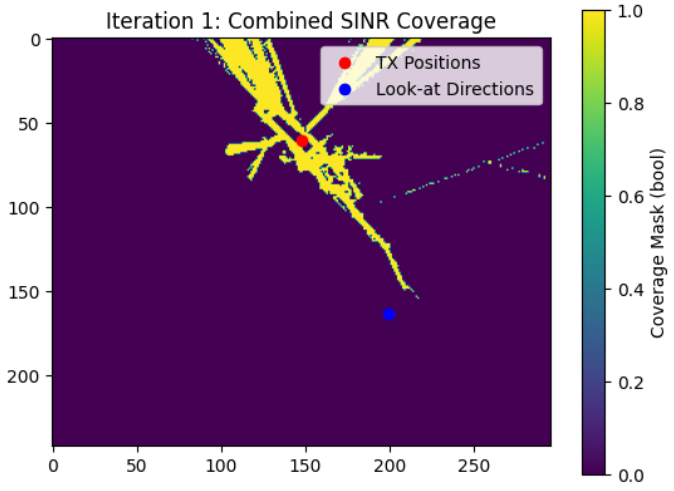

Fig. 19. Theoretical SINR coverage of MISO Dynamically Uniform Distributed 2TX at first iteration, TX Height = 20m

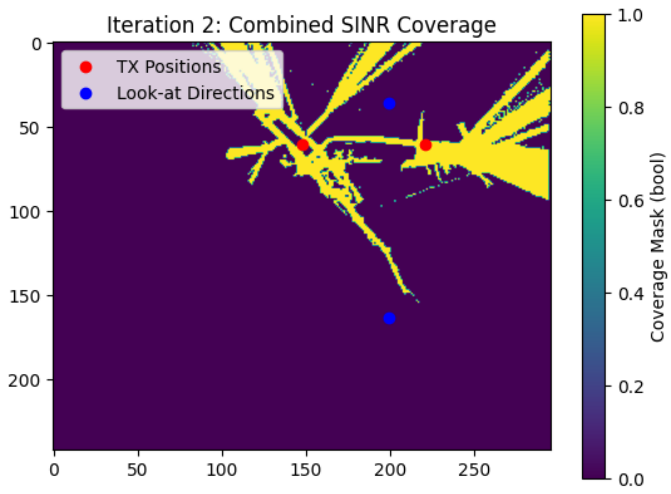

Fig. 20. Theoretical SINR coverage of MISO Dynamically Uniform Distributed 2TX at second iteration, TX Height = 20m

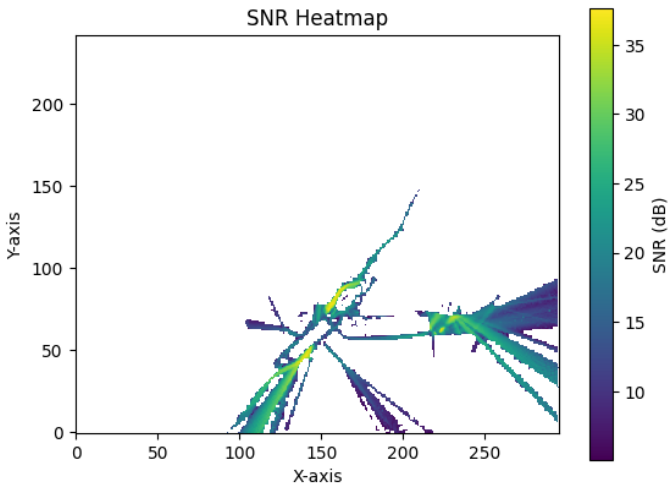

Fig. 21. FINAL SINR coverage of MISO Uniform Dynamically Distributed 2TX from Sionna, TX Height = 20m

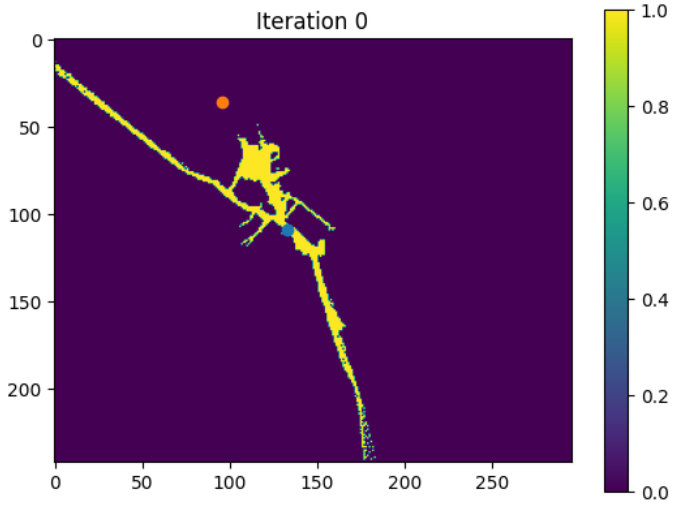

Fig. 22. Theoretical SINR coverage of MISO Centralized 4TX at first iteration, TX Height = 20m

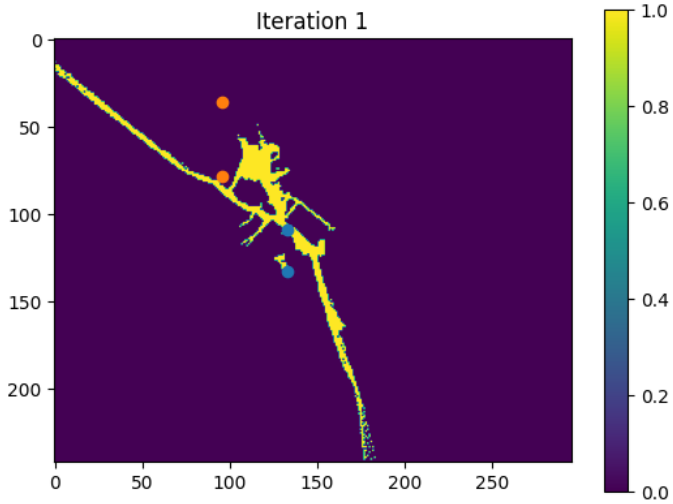

Fig. 23. Theoretical SINR coverage of MISO Centralized 4TX at second iteration, TX Height = 20m

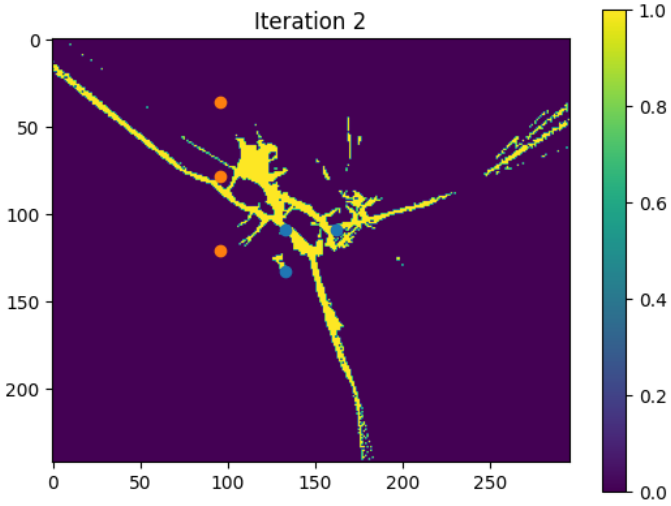

Fig. 24. Theoretical SINR coverage of MISO Centralized 4TX at third iteration, TX Height = 20m

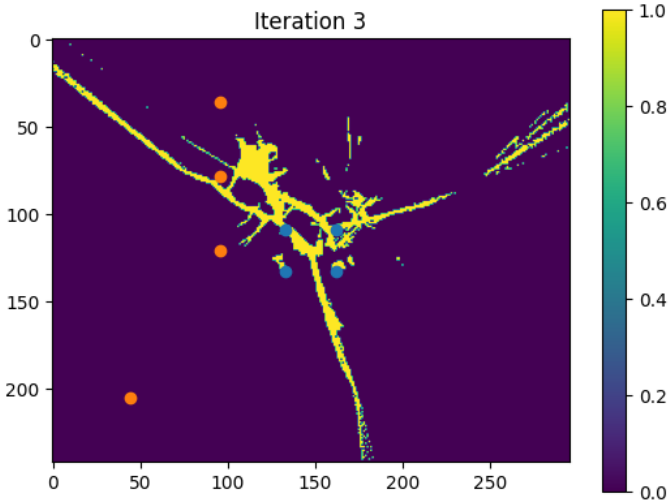

Fig. 25. Theoretical SINR coverage of MISO Centralized 4TX at fourth iteration, TX Height = 20m

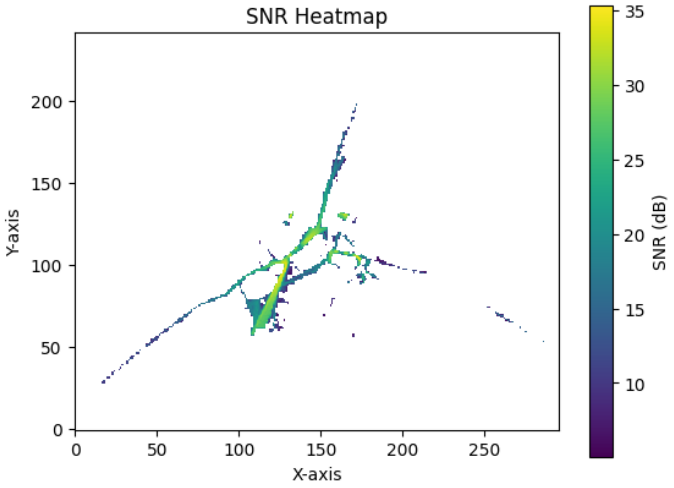

Fig. 26. FINAL SINR coverage of MISO Centralized 4TX from Sionna, TX Height = 20m

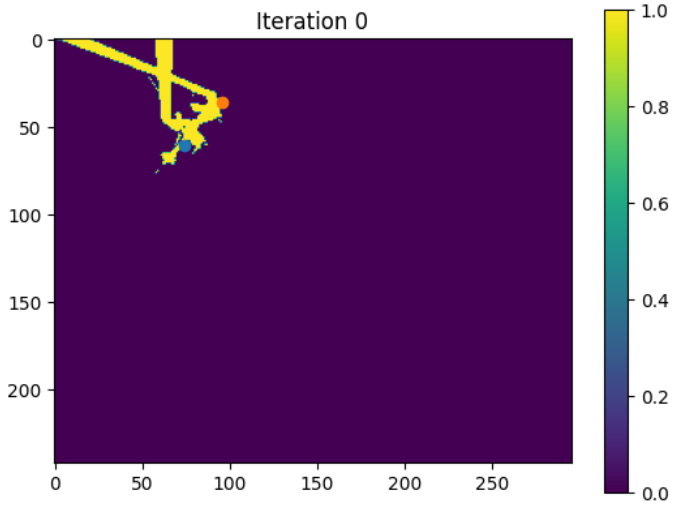

Fig. 27. Theoretical SINR coverage of MISO Uniform Distributed 4TX at first iteration, TX Height = 20m

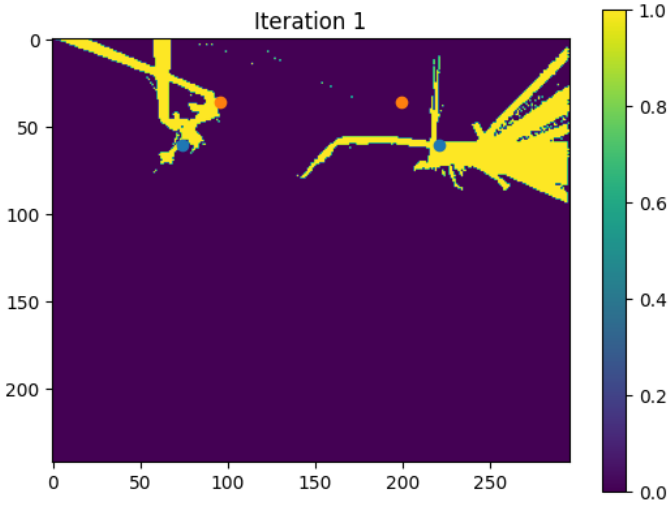

Fig. 28. Theoretical SINR coverage of MISO Uniform Distributed 4TX at second iteration, TX Height = 20m

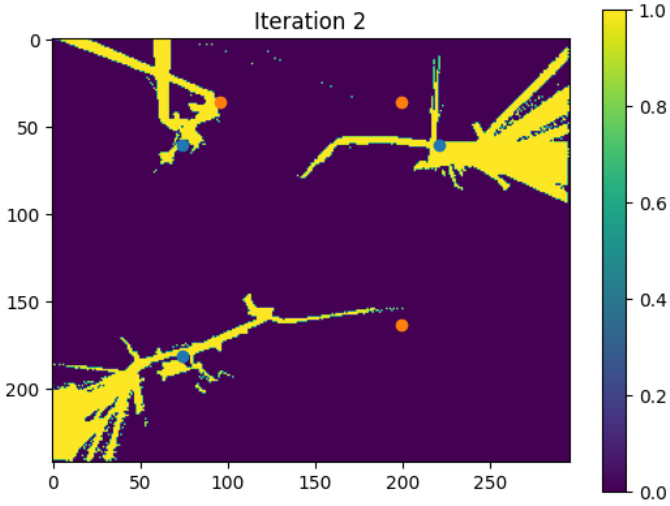

Fig. 29. Theoretical SINR coverage of MISO Uniform Distributed 4TX at third iteration, TX Height = 20m

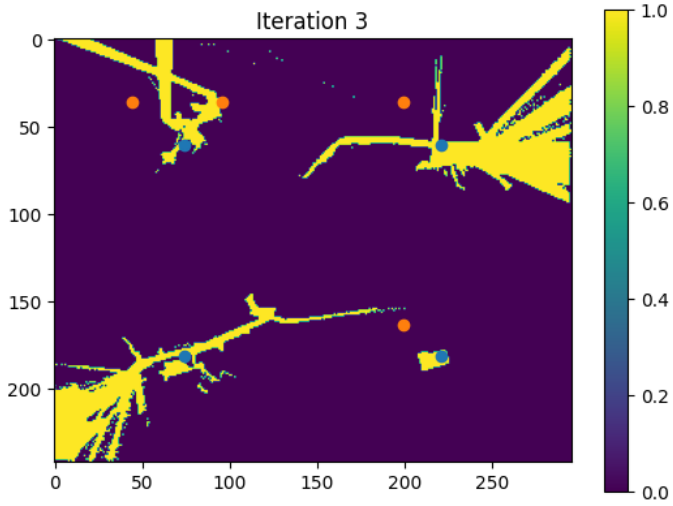

Fig. 30. Theoretical SINR coverage of MISO Uniform Distributed 4TX at fourth iteration, TX Height = 20m

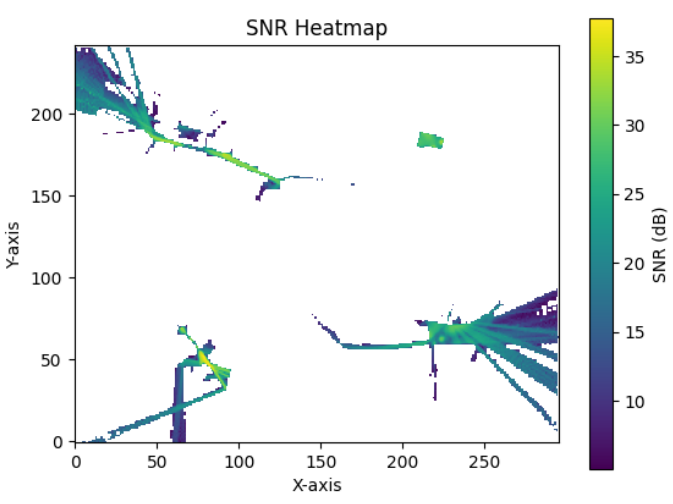

Fig. 31. FINAL SINR coverage of MISO Uniform Distributed 4TX from Sionna, TX Height = 20m

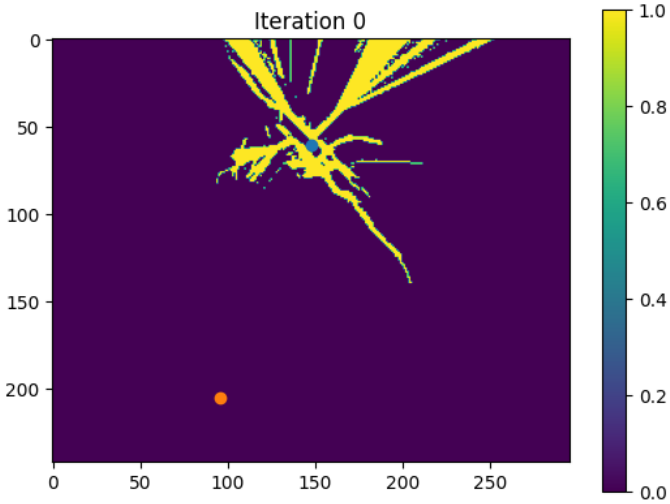

Fig. 32. Theoretical SINR coverage of MISO Dynamically Uniform Distributed 4TX at first iteration, TX Height = 20m

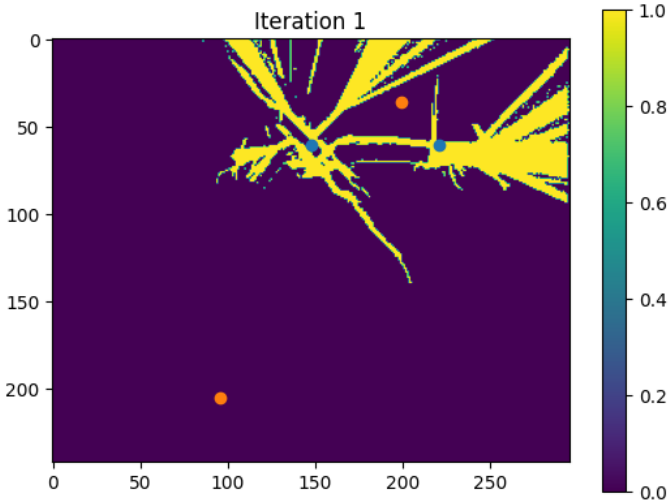

Fig. 33. Theoretical SINR coverage of MISO Dynamically Uniform Distributed 4TX at second iteration, TX Height = 20m

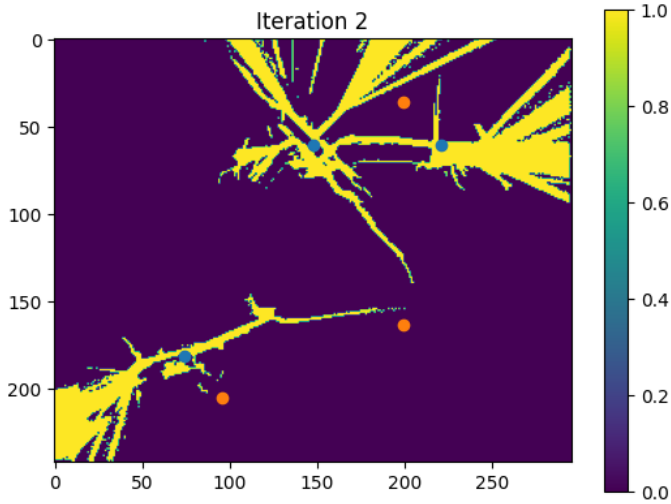

Fig. 34. Theoretical SINR coverage of MISO Dynamically Uniform Distributed 4TX at third iteration, TX Height = 20m

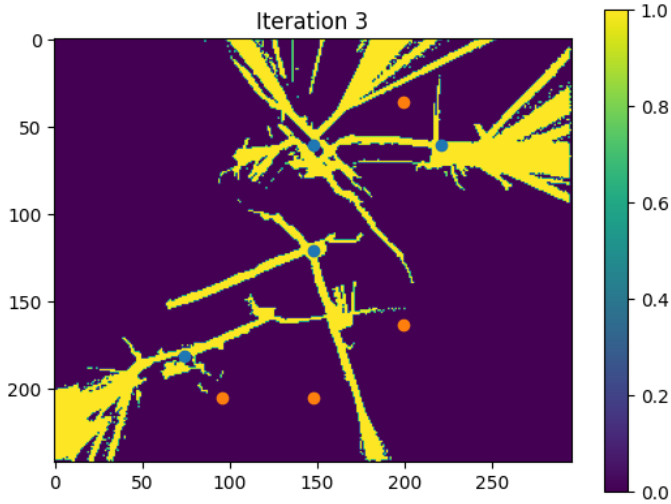

Fig. 35. Theoretical SINR coverage of MISO Dynamically Uniform Distributed 4TX at fourth iteration, TX Height = 20m

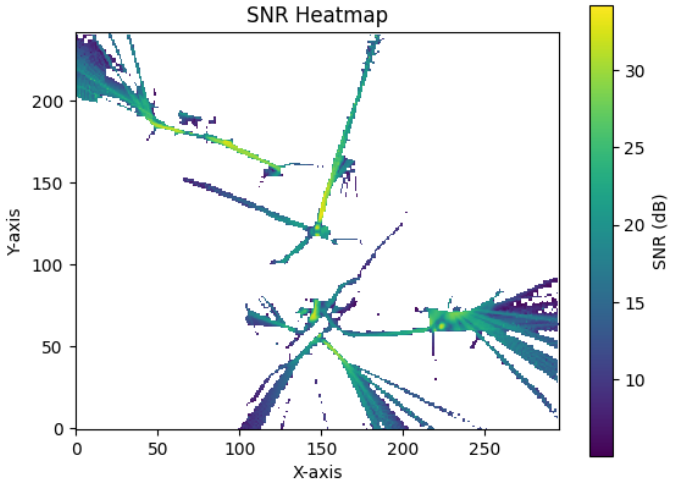

Fig. 36. FINAL SINR coverage of MISO Dynamically Uniform Distributed 4TX from Sionna, TX Height = 20m